Journal of Pure and Applied Mathematics: Advances and Applications
Volume 9, Number 2, 2013, Pages 81-106

NUMERICAL STUDY OF PULSATILE BLOOD FLOW IN THE CORONARY SYSTEM WITH THE RCA BYPASS GRAFT

BURASKORN NUNTADILOK, JULIAN POULTER, PICHIT BOONKRONG and BENCHAWAN WIWATANAPATAPHEE

Department of Mathematics
Faculty of Science
Mahidol University
Bangkok 10400
Thailand
e-mail: julian.pou@mahidol.ac.th
benchawan.wiw@mahidol.ac.th

Abstract

In this work, we investigate the pulsatile blood flow in the human coronary artery system with no graft and with a bypass graft. The computational domain consists of the ascending aorta, the aortic arch, the proximal left coronary artery (LCA), the right coronary artery (RCA), and a graft. Blood is assumed to be an incompressible non-Newtonian fluid. The motion of blood flow is governed by the continuity equation and the Navier-Stokes equations with pulsatile conditions on the boundaries. The governing equations are solved by using the finite element method. Disturbances of blood flow through the stenosed RCA with no graft and with a bypass graft for the degree of stenotic flow restrictions 50%, 63%, and 72% are investigated. The numerical results show that the blood pressure drops dramatically, the shear rate tends to increase in the stenosis area, and the maximal RCA flow decreases as the degree of stenosis increases. Additionally, the

2010 Mathematics Subject Classification: 74S05, 76D05, 93C20.

Keywords and phrases: blood flow, coronary artery bypass graft, incompressible non-Newtonian fluid, stenosis.

Received February 8, 2013

results also show that the coronary artery system with a bypass graft can increase the maximal flow in the stenosed RCA, improve the blood pressure, and decrease the shear rate in the stenosis region.

1. Introduction

Cardiovascular diseases (CVDs), a group of disorders of the heart and blood vessels, are considered as a major cause of human death in the world. In 2008, World Health Organization (WHO) reported that about 17.3 million people died because of CVDs [27]. Recently, WHO has predicted that almost 23.6 million people may die from CVDs in 2030. Interestingly, it is realized that most of the cases are associated with some form of abnormal blood flow in the blocked coronary arteries, which is believed to be a significant factor at the onset of coronary heart diseases. To deal with this problem, there are many practical ways to treat coronary artery disease (CAD) including drugs, stent replacement, and coronary artery bypass grafting. A doctor may use drugs for a patient, who has a degree of stenosis less than 70% that does not severely limit the flow of blood [26]. A coronary angioplasty and stent placement is suitable for a patient with a high risk of an open-heart surgery, and other cases with severe stenosis, coronary artery bypass grafting (CABG) is suitable. Figure 1 displays a system of coronary arteries with grafts. In this study, we focus on surgical treatment of CABG, which is used worldwide each year. However, up to 25% of grafts fail within one year and up to 50% fail within ten years after surgery [3, 17]. Recently, it has been recognized that success of bypass surgery depends on many factors, such as the information of rheological behaviour of blood, the pressure distribution, the flow speed, and wall shear stress in the stenosed coronary artery before and after surgery.

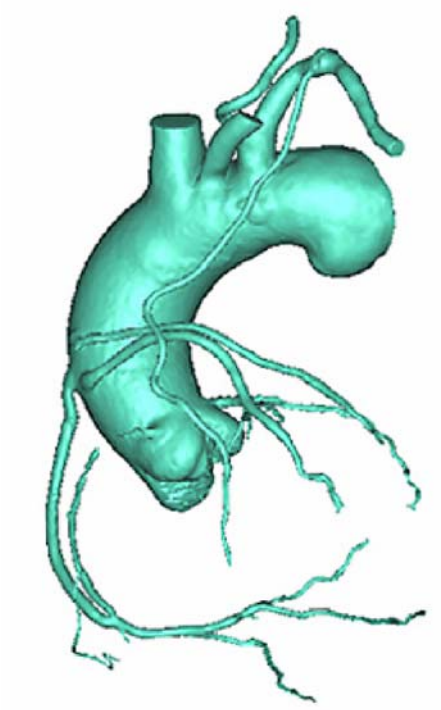

Figure 1. The real geometry of coronary artery system with bypass grafts.

A number of in-vivo and vitro experiments have been conducted to overcome the problem of the pathogenesis of coronary diseases by using animal models [20]. Due to the difficulty and limitation in determining the critical flow conditions for both in-vivo and vitro experiments, the exact mechanism involving CABG is not well understood. Mathematical modelling and numerical simulation are thus chosen to be a better way to study this problem. Over the last two decades, various mathematical models have been proposed to describe the rheological behaviour of blood in a normal artery [1, 2, 4, 9, 14, 15, 16, 23], a stenosed artery [6, 8, 11, 12, 15, 19, 21, 24], and a coronary artery bypass graft [5, 7, 10, 13, 22, 25]. Bertolotti and Deplano [10] studied the blood flow patterns at the anastomosis of a stenosed coronary bypass by using a stenosed straight tube with a graft. Their results pointed out that different flow rates and distances between the anastomosis and the stenosis throat give different

flow patterns. Papaharilaou et al. [25] studied the effect of the pulsatile blood flow in a distal end-to-side anastomosis. The domain used in this work was a straight tube with both a planar and non-planar graft. They found that the magnitude of mean oscillatory shear in the non-planar domain was reduced as compared to the planar domain. Siddiqui et al. [24] studied the effects of pulsatile blood flow through a stenosed artery by using a straight tube with a stenosis region. From their study, the mean and steady flow rates decrease as the yield stress increases. It is notable that the studies mentioned above used unreal geometries of coronary arteries such as straight and curve tubes, and unrealistic conditions such as constant velocity at the inlet and constant pressure at the outlet. Wiwatanapataphee et al. [7] studied the behaviour of pulsatile blood flow in a stenosed coronary artery with a bypass graft by using realistic boundary conditions whilst the domain was unreal. The effect of bypass graft angle on the flow pattern was investigated. It was found that different bypass angles gave different flow patterns. Chuchard et al. [19] studied the behaviour of blood flow through the system of coronary arteries with stenosis of the left anterior descending by using realistic domain. Their simulation results showed that the blood flows with high speed had pressure rapidly dropping in the stenosis area. Wiwatanapataphee et al. [9] studied the effect of branching on blood flow in the system of coronary arteries by using pulsatile flow condition on the boundary and a realistic geometry of human coronary arteries. The results indicated that the blood pressure in the coronary system with branching vessels is lower than the one in the coronary system with no branch, and the wall shear stress at bifurcation is higher than a nearby region.

In this study, we consider the flow of blood through the system of coronary arteries with no graft and with a bypass graft. We extend our previous works [5] and [9]. The computational domains are constructed based on computed tomography (CT) scans of patients coronary arteries by using Mimic software. The domain includes the ascending aorta, the arch of aorta, the proximal LCA, the RCA, and a graft. The rest of this

paper is organized as follows. In Section 2, the mathematical model and finite element formulation of the blood flow are explained. After that, the results of numerical simulations for the flow through the coronary system with no graft and with a bypass graft are presented in Section 3 and some conclusions are presented in Section 4.

2. Mathematical Model

2.1. Governing equations

The transient phenomena of blood flow through the system of coronary arteries are governed by the continuity equation (1) and Navier-Stokes equations (2):

$$\nabla \cdot \vec{u} = 0, \tag{1}$$

$$\rho\left[\frac{\partial \vec{u}}{\partial t} + (\vec{u} \cdot \nabla)\vec{u}\right] = \nabla \cdot \sigma, \tag{2}$$

where $\vec{u}$ denotes the velocity vector, ρ is the density of blood, and σ is the total stress tensor described by

$$\sigma = -pI + \eta(\dot{\gamma})[\nabla\vec{u} + (\nabla\vec{u})^T]. \tag{3}$$

In Equation (3), p represents the blood pressure, I is 3 × 3 identity matrix, $\eta(\dot{\gamma})$ is the viscosity of blood, and $\dot{\gamma}$ is the shear rate. Blood is assumed to be a non-Newtonian fluid and the blood viscosity is described by the Carreau model:

$$\eta(\dot{\gamma}) = \eta_\infty + (\eta_0 - \eta_\infty)[1 + (\lambda\dot{\gamma})^2]^{(n-1)/2}, \tag{4}$$

where the parameters $\eta_0 = 0.56\text{g/cm}^3$, $\eta_\infty = 0.0345\text{g/cm}^3$, $\lambda = 3.313\text{s}$, and $n = 0.3568$ and the shear rate $\dot{\gamma}$ is defined by

$$\dot{\gamma} = \sqrt{2tr[\frac{1}{2}(\nabla\vec{u} + (\nabla\vec{u})^T)]^2}. \tag{5}$$

Moreover, pulsatile conditions of the flow rate and the pressure are applied on the boundaries. We assume that the pulsatile pressure and flow rate have no difference in a variation of time. Thus, the pulsatile pressure and flow rate can be expressed by the periodic functions $p(t) = p(t + mT)$ and $Q(t) = Q(t + mT)$ for $m = 0, 1, 2, \ldots$ and T denotes the cardiac period. Mathematically, the pulsatile pressure and flow rate can be approximated by the truncated Fourier series by using experimental data [8].

$$p(t) = \overline{p} + \sum_{k=1}^{4} \alpha_k^p \cos(k\omega t) + \beta_k^p \sin(k\omega t), \tag{6}$$

$$Q(t) = \overline{Q} + \sum_{k=1}^{4} \alpha_k^Q \cos(k\omega t) + \beta_k^Q \sin(k\omega t), \tag{7}$$

where $\overline{p}$ is the mean pressure, $\overline{Q}$ is the mean flow rate, and $\omega = 2\pi / T$ is an angular frequency with period T. The values of α_k^Q, β_k^Q, α_k^p, and β_k^p are given in Table 1.

Table 1. Values of the parameters α_k^Q, β_k^Q, α_k^p, and β_k^p

Vessel	k	α_k^Q	β_k^Q	α_k^p	β_k^p
Aorta	1	1.7048	– 7.5836	8.1269	– 12.4156
	2	– 6.7035	– 2.1714	– 6.1510	– 1.1072
	3	– 2.6389	2.6462	– 1.3330	– 0.3849
	4	0.7198	0.2687	– 2.9473	1.1603
LCA	1	0.1007	0.0764	– 3.3107	– 2.2932
	2	– 0.0034	– 0.0092	– 9.8639	8.0487
	3	0.0294	0.0337	3.0278	3.8009
	4	0.0195	– 0.0129	2.2476	– 3.2564
RCA	1	0.0393	0.0241	5.9369	3.6334
	2	– 0.0360	0.0342	– 11.1990	2.1255
	3	– 0.0131	0.0026	– 2.2778	– 3.7528
	4	– 0.0035	– 0.0041	2.7333	– 0.6375

On the inlet surface of the aorta ($\Gamma_{\text{in}}^{\text{aorta}}$), we set the pulsatile velocity

$$\vec{u}_{\text{in}}(t) = \frac{Q(t)}{A}, \tag{8}$$

where $A = 6.88\text{cm}^2$ is the cross-sectional area of the inlet boundary. On the outlet surfaces including Γ_1^{aorta}, Γ_2^{aorta}, Γ_3^{aorta}, Γ_4^{aorta}, Γ_1^{RCA}, Γ_2^{RCA}, Γ_3^{RCA}, Γ_4^{RCA}, Γ_1^{LCA}, and Γ_2^{LCA}, we impose the corresponding pulsatile pressure condition:

$$\sigma \cdot \vec{n} = -p(t)\vec{n}. \tag{9}$$

A no-slip condition is applied to the arterial wall such that

$$\vec{u} = \vec{0}. \tag{10}$$

In summary, the blood flow problem in the system of human coronary arteries is governed by the boundary value problem (BVP). That is to find $\vec{u}$ and p such that Equations (1)-(5) and all boundary conditions (6)-(10) are satisfied.

2.2. Finite element formulation

Using the total weighted residual method with the system of Equations (1)-(2), we obtain the variational statement corresponding to the BVP. That is to find $\vec{u} \in [H^1(\Omega)]^3$ and $p \in H^1(\Omega)$ such that for all $\vec{w}^u \in [H_0^1(\Omega)]^3$ and $w^p \in H_0^1(\Omega)$, all boundary conditions are satisfied and

$$(\nabla \cdot \vec{u},\, w^p) = 0, \tag{11}$$

$$\rho\left(\frac{\partial \vec{u}}{\partial t},\, \vec{w}^u\right) + \rho((\vec{u} \cdot \nabla)\vec{u},\, \vec{w}^u) = (\nabla \cdot \sigma,\, \vec{w}^u), \tag{12}$$

where $H^1(\Omega)$ is the Sobolev space $W^{1,2}(\Omega)$ with norm $\|\cdot\|_{1,2,\Omega}$, $H_0^1(\Omega) = \{v \in H^1(\Omega) | v = 0$ on the Dirichlet type boundary$\}$, and $(\cdot,\cdot)$ denotes the inner product of the square integrable function space $L^2(\Omega)$.

By using the boundary conditions (8) and (10) and applying the Galerkin finite element method, we then obtain the following system:

$$C^T U = 0, \tag{13}$$

$$M\dot{U} + A_u(u)U + \widetilde{C}P = 0, \tag{14}$$

where $U = (\vec{u}_1, \vec{u}_2, \vec{u}_3, \ldots, \vec{u}_k, \ldots, \vec{u}_N)$ with $\vec{u}_k$ is the velocity vector at the k-th finite element node. The matrices C, M, $A_u(u)$, and $\widetilde{C}$ are derived in the Galerkin finite element formulation. To find the finite element solutions, we use the backward Euler difference scheme with a typical time step $t_n \to t_{n+1}$. We then have $\dot{U} = (U_{n+1} - U_n)/\Delta t_n$ and

$$C^T U_{n+1} = 0, \tag{15}$$

$$\frac{M}{\Delta t_n} U_{n+1} + A_u(u)U_{n+1} - \widetilde{C}P_{n+1} = \frac{M}{\Delta t_n} U_n, \tag{16}$$

which is a nonlinear system because $A_u(u)$ in Equation (16) depends on U_{n+1}. The iterative process stops when

$$\|U_{n+1} - U_n\| < 0.001 \text{ and } \|P_{n+1} - P_n\| < 0.001.$$

3. Numerical Examples

We have simulated the three-dimensional blood flow through the system of human coronary arteries with no graft and with a bypass graft. The domains based on a real geometry of the coronary artery system are constructed by using 349 images of computed tomography scans. The computational domain of the coronary artery system consists of the ascending aorta, the aortic arch, the proximal LCA, the RCA with

stenosis region, and the graft connected between ascending aorta and the RCA, as shown in Figure 2. The stenosis area is at 1.3cm from the RCA connected to the base of the aorta. The graft is connected from the ascending aorta to the RCA at 8.4cm from the RCA inlet. The properties of the computational domain used in this study are given in Table 2.

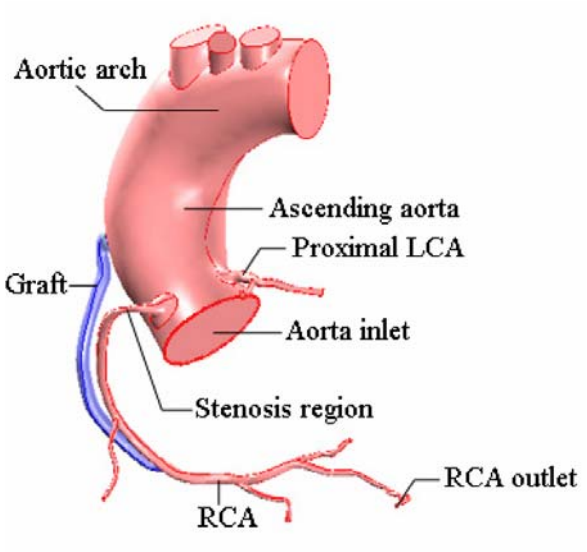

Figure 2. The computational domain of the system of coronary arteries with a bypass graft.

Table 2. The properties of the computational domain

	Volume (cm^3)	Surface area (cm^2)	Perimeter (cm)	Length (cm)
The domain with no graft	82.774	–	–	–
The domain with a bypass graft	83.765	–	–	–
A graft	0.991	10.013	–	8.101
The main RCA	–	–	–	18.699
Γ_{in}^{aorta}	–	6.882	9.318	–

At the beginning, two finite element meshes including the coronary artery system with no graft and with a bypass graft are created as shown

in Figure 3. In our simulation, we use the density of human blood of 1.06g/cm^3 [11]. The mean flow rates $\overline{Q}$ of the aorta, the LCA, and the RCA are $95.37\text{cm}^3 \cdot \text{s}^{-1}$, $2.648\text{cm}^3 \cdot \text{s}^{-1}$, and $1.493\text{cm}^3 \cdot \text{s}^{-1}$, respectively. The mean pressure $\overline{p}$ of the aorta, the LCA, and the RCA are, respectively, 97.22mmHg, 65.97mmHg, and 65.33mmHg and the period of heart pump is $T = 0.8\text{s}$.

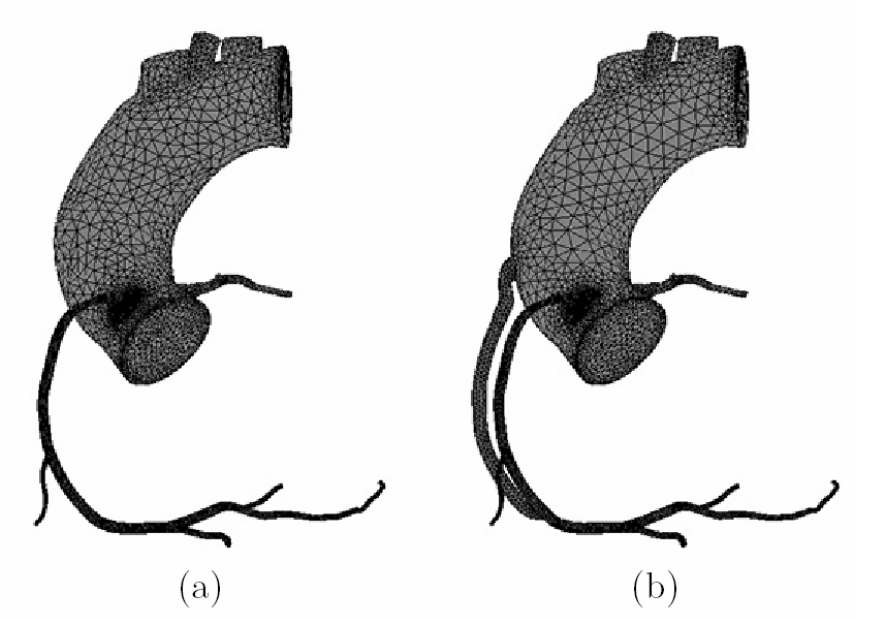

Figure 3. Two domain meshes of the system of coronary arteries: (a) with no graft and (b) with a bypass graft.

Throughout the simulation, various degrees of stenosis are introduced at the proximal RCA. The effects of four different degrees of stenosis including 0%, 50%, 63%, and 72%, and the effects of bypass graft are investigated. Figure 4 displays the main RCA, the RCA axis, and the RCA outlet surface, where the pressure, velocity, and shear rate are discussed. Figure 5 displays the pressure distribution in the coronary artery system with no graft. The results show that the stenosis increases the pressure drop at the stenosis site. This causes the lower pressure appearing along the RCA having various degrees of stenosis. Figure 6 presents the

pressure profile along the RCA axis at the peak of systole and diastole. The results indicate that the higher degree of stenosis, the more likely the pressure drop appears at the stenosis area.

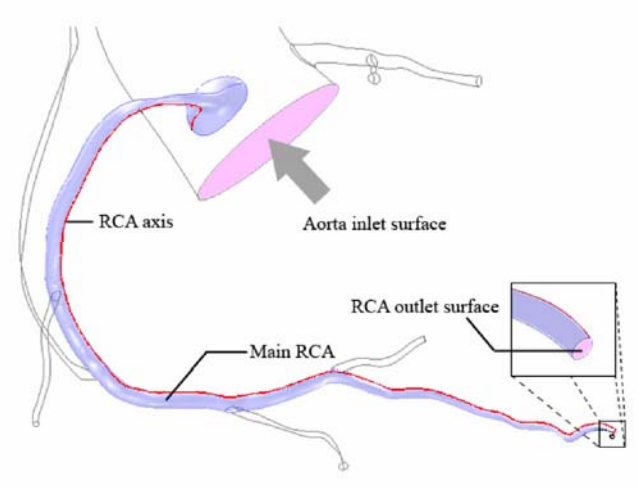

Figure 4. The investigated axis of the RCA, the main RCA, and the RCA outlet surface.

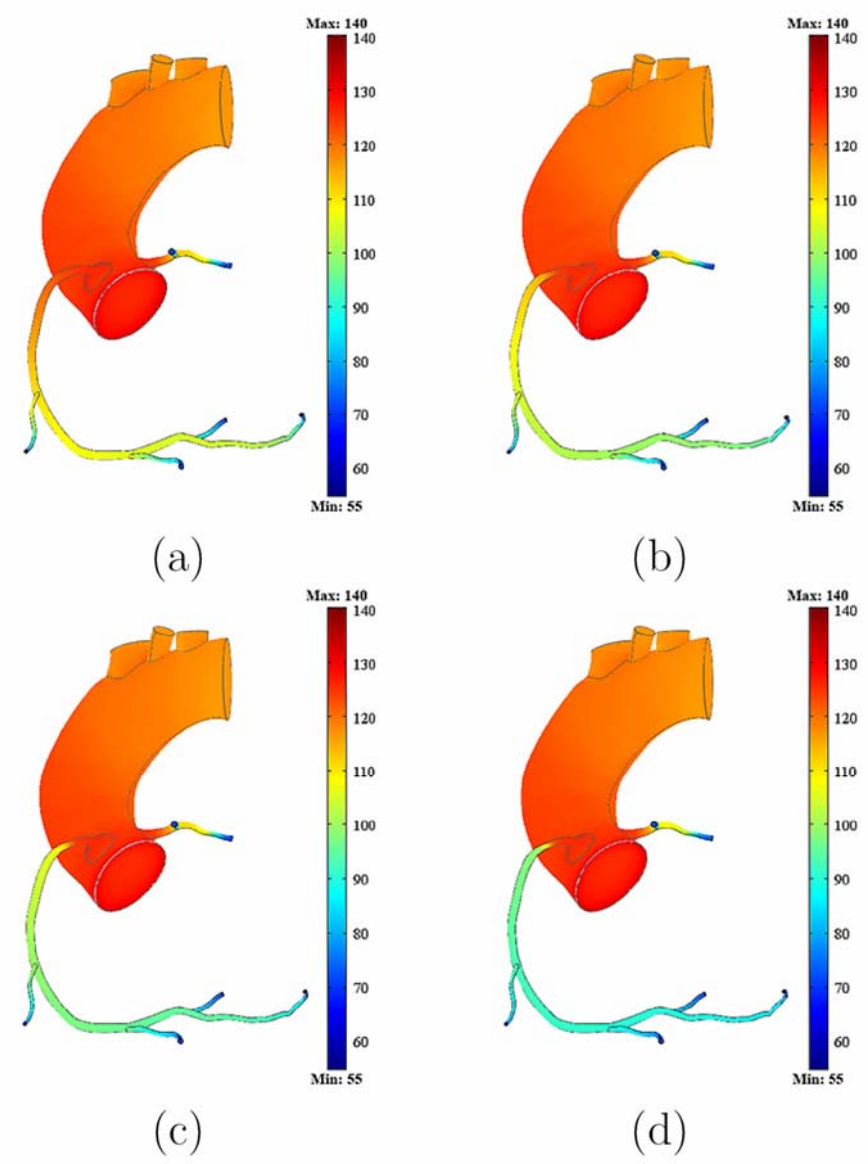

Figure 5. The pressure distribution of the coronary artery system with stenosed RCA having different degrees of stenosis: (a) 0%; (b) 50%; (c) 63%; and (d) 72% at the peak of systole.

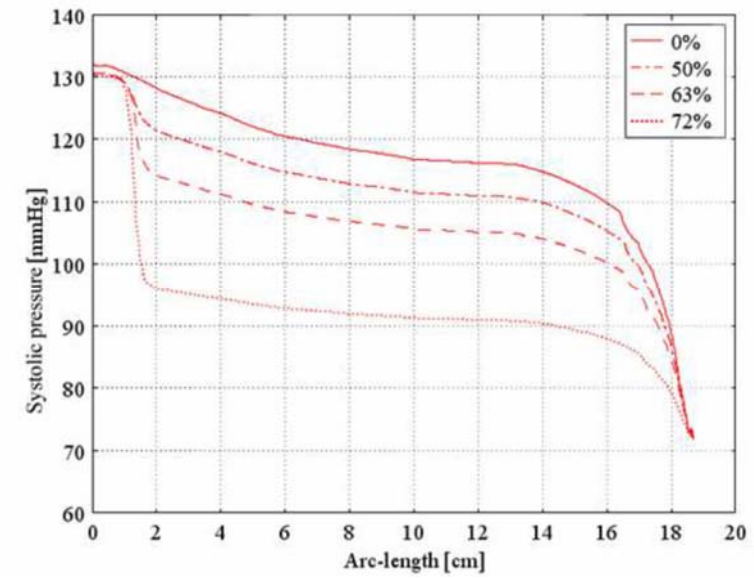

(a)

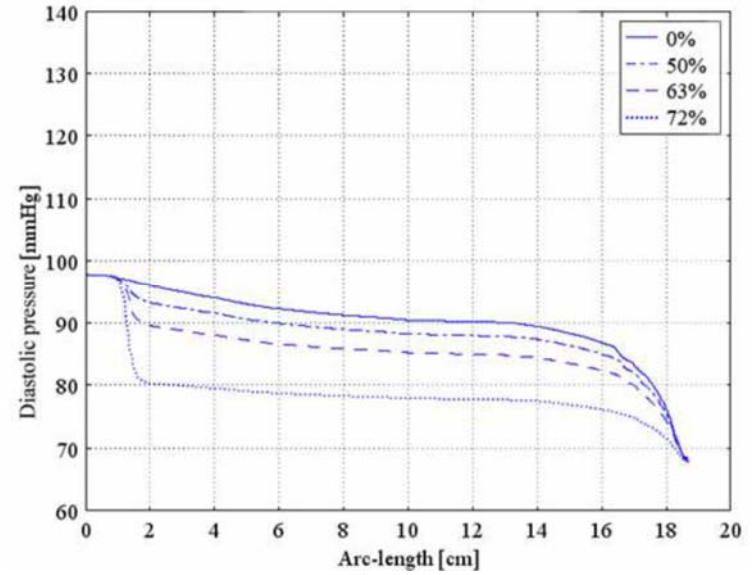

(b)

Figure 6. The pressure profile along the RCA axis obtained from the model with stenosed RCA having different degrees of stenosis: 0% (solid line); 50% (dash-dot line); 63% (dashed line); and 72% (dotted line) at two different times: (a) the peak of systole and (b) the peak of diastole.

We further consider the pressure along the RCA axis and the pressure distribution in the coronary artery system with a bypass graft. Figure 7 shows the comparison of pressure in the coronary artery system with no graft and with a bypass graft. It indicates that blood pressure along the stenosed RCA increases after the bypass grafting. As shown in Figure 8, the pressure profile obtained from the model with a bypass graft increases along the axis of RCA at the peak of systole and diastole. We can conclude that the CABG can reduce the pressure drop in the stenosis region.

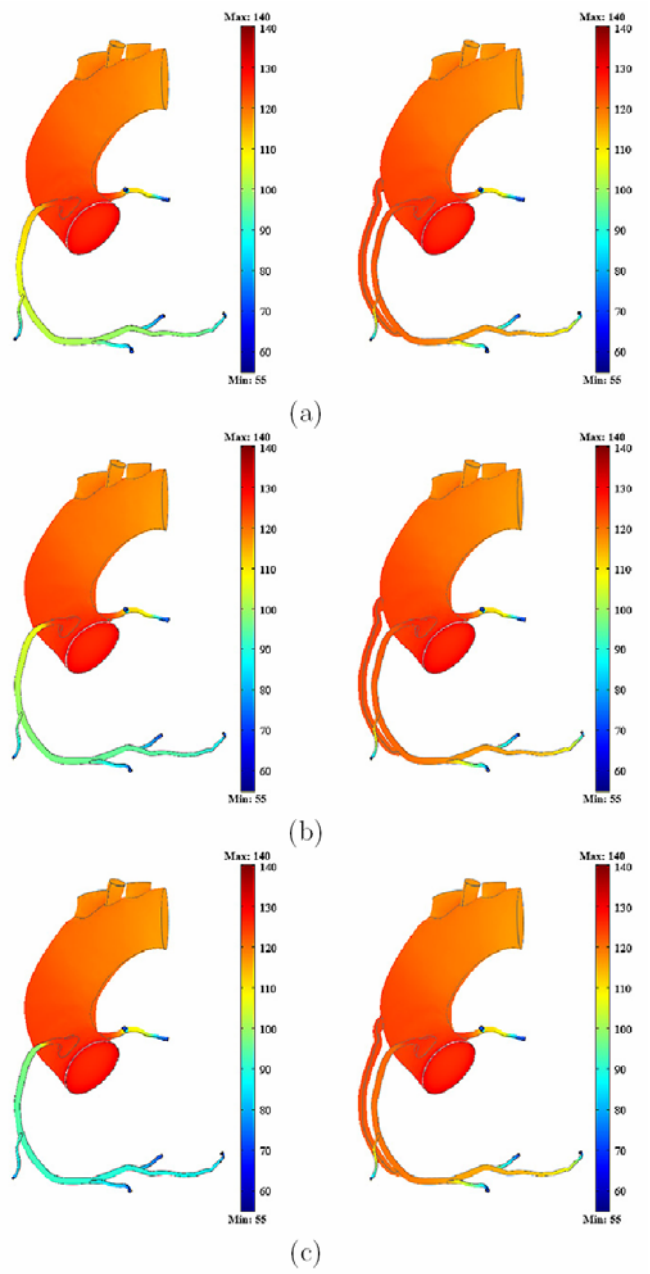

Figure 7. The pressure distribution of the coronary artery system with stenosed RCA with no graft (left)/with a bypass graft (right) having different degrees of stenosis: (a) 50%; (b) 63%; and (c) 72% at the peak of systole.

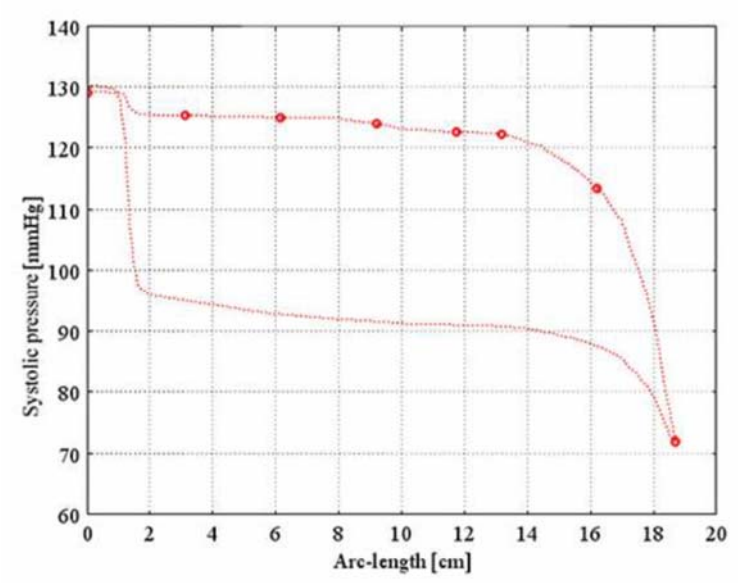

(a)

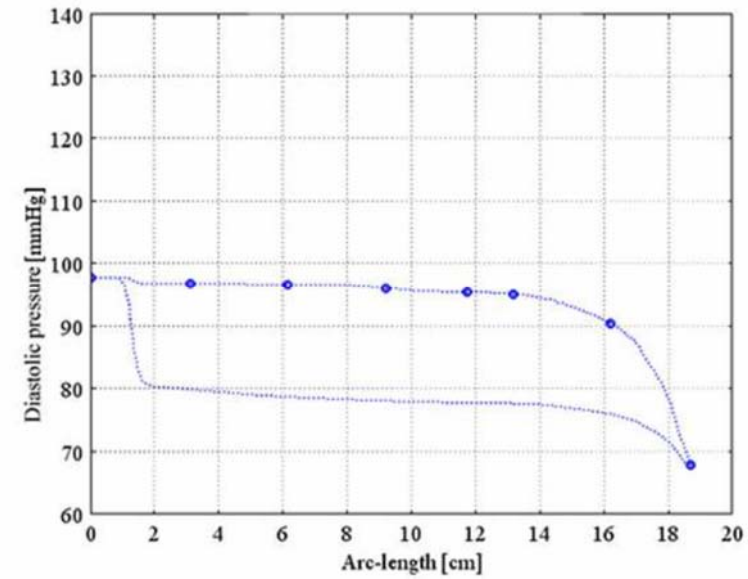

(b)

Figure 8. The pressure profile along the RCA axis obtained from the model with 72% RCA stenosis with no graft (dotted line) and with a bypass graft (dotted line with circle) at two different times: (a) the peak of systole and (b) the peak of diastole.

Figure 9 shows the maximal flow at the outflow surface of the main RCA having different degrees of stenosis. It is noted that the higher degree of stenosis gives lower maximal flow at the RCA outlet surface. The influence of the bypass graft on the RCA maximal flow is also investigated. The results indicate that the bypass graft has significant effect on the RCA maximal flow. The coronary artery system with a bypass graft increases the maximal flow, comparison with the one with no graft. Figures 10 and 11 show that bypass grafting is able to increase the velocity field at the RCA outlet surface.

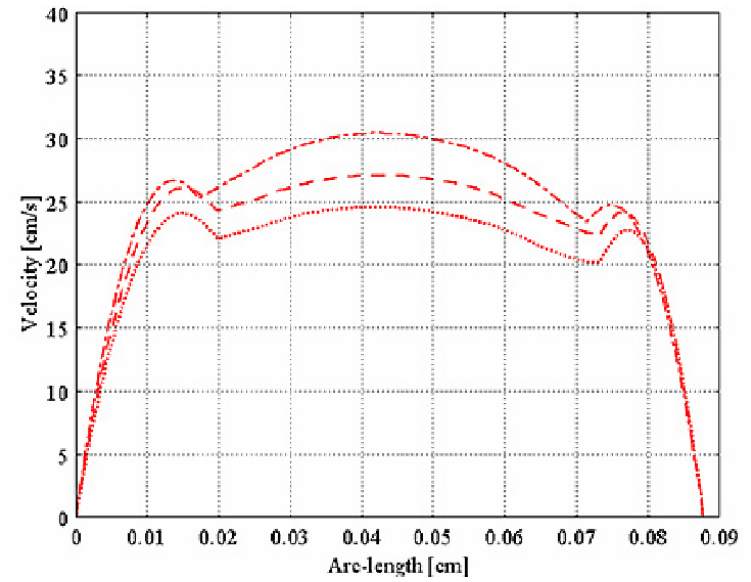

(a)

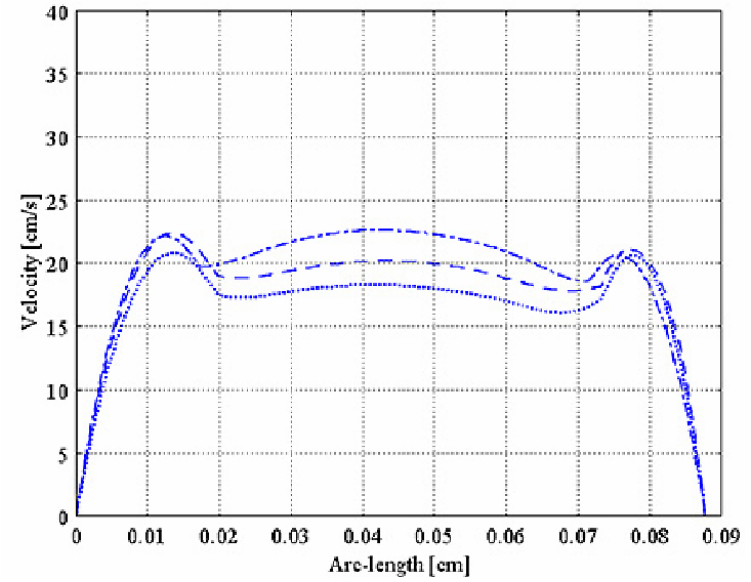

(b)

Figure 9. The maximal flow obtained from the model with stenosed RCA having different degrees of stenosis: 50% (dash-dot line); 63% (dashed line); and 72% (dotted line) at two different times: (a) the peak of systole and (b) the peak of diastole.

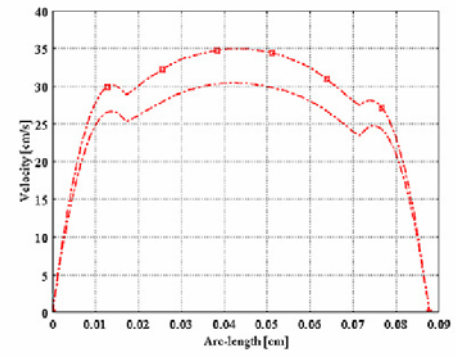

(a)

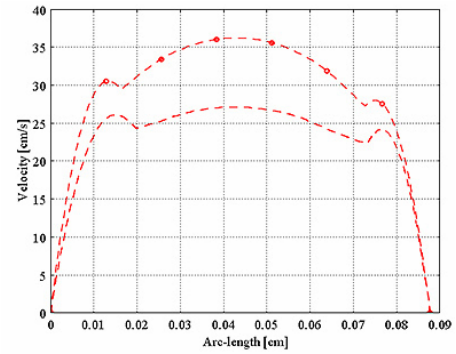

(b)

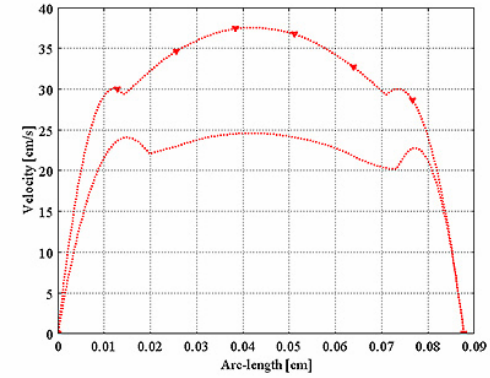

(c)

Figure 10. The RCA maximal flow obtained from the model with no graft (line below) and with a bypass graft (line above) having different degrees of stenosis: (a) 50%; (b) 63%; and (c) 72% at the peak of systole.

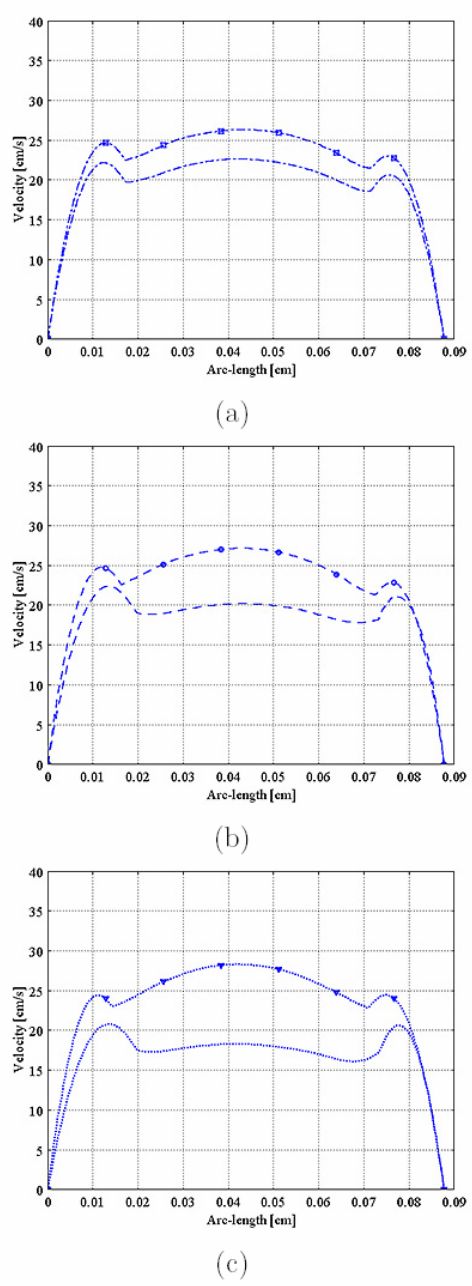

Figure 11. The RCA maximal flow obtained from the model with no graft (line below) and with a bypass graft (line above) having different degrees of stenosis: (a) 50%; (b) 63%; and (c) 72% at the peak of systole.

In addition, we investigate the effect of the stenosis degree on the shear rate along the RCA axis. Figure 12 shows the results obtained from the stenosed RCA in the coronary system with no graft. It shows that the shear rate tends to increase as the degree of stenosis increases at the stenosis site. Figure 13 shows the shear rate along the RCA axis obtained from the model with 72% RCA stenosis at two conditions: model with no graft and with a bypass graft. The results show that the shear rate decreases from 3841 s^{-1} to 1035 s^{-1} at the peak of systole and from 2834 s^{-1} to 690 s^{-1} at the peak of diastole at the stenosis site after the bypass grafting.

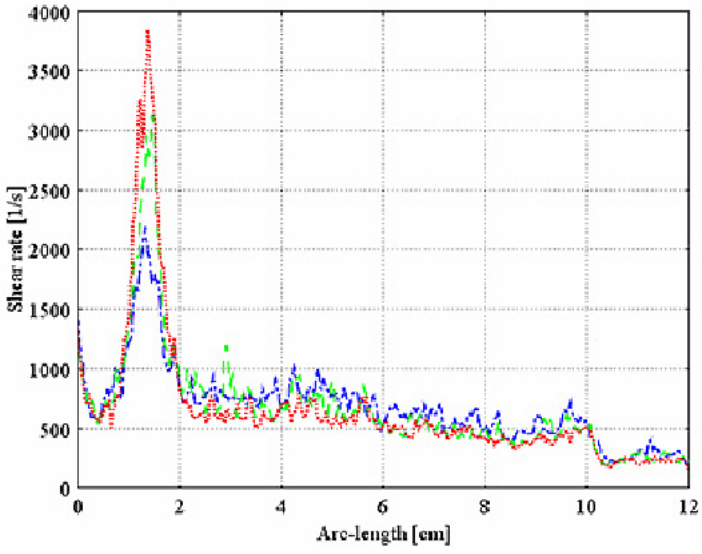

(a)

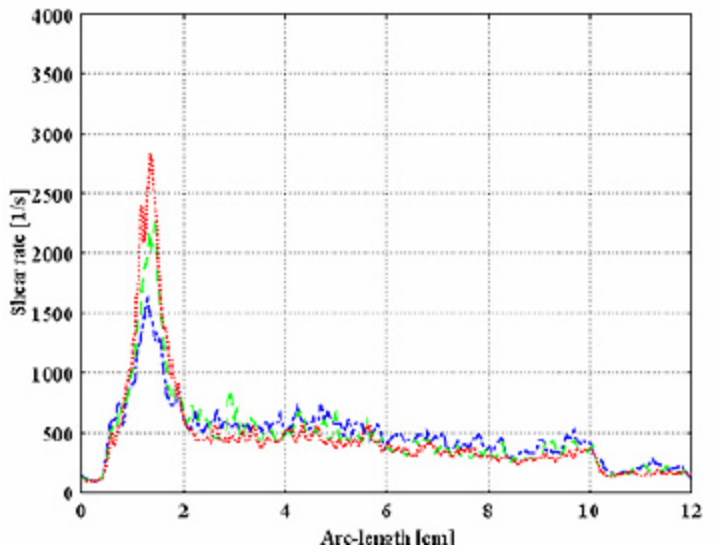

(b)

Figure 12. The shear rate along 12cm of the RCA axis obtained from the coronary artery system having different degrees of RCA stenosis: 50% (dash-dot line); 63% (dashed line); and 72% (dotted line) at two different times: (a) the peak of systole and (b) the peak of diastole.

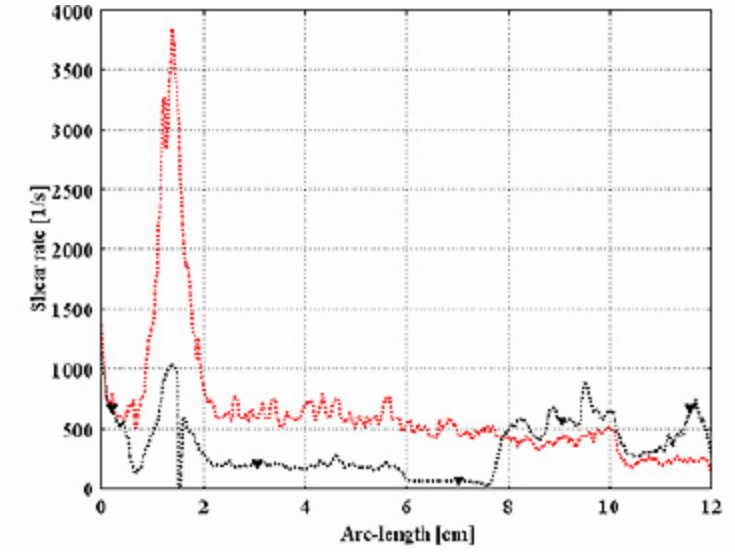

(a)

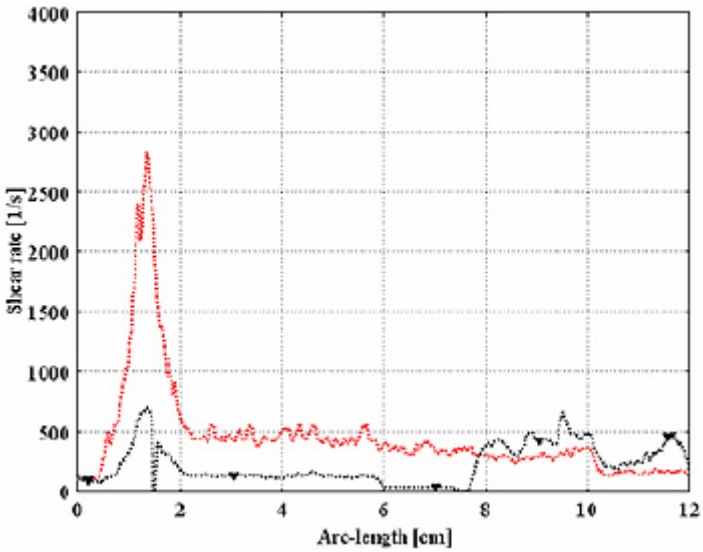

(b)

Figure 13. The shear rate along 12cm of the RCA axis obtained from the coronary artery system with 72% RCA stenosis with no graft (dotted line) and with a bypass graft (dotted line with triangle) at two different times: (a) the peak of systole and (b) the peak of diastole.

4. Conclusion

In this work, we present the numerical results of blood flow through the system of coronary arteries with no graft and with a bypass graft under the pulsatile conditions. The effects of the stenosis degree and bypass grafting on the flow problem are investigated. It is found that the blood pressure drops dramatically in the stenosis region and the velocity at the RCA outflow decreases as the degree of stenosis increases. In the domain of the coronary system with a bypass graft, the velocity field increases and the blood pressure and the shear rate, especially at stenosis area, are better than those obtained from the model with no graft.

Acknowledgement

The authors would like to thank for the financial support provided by the Faculty of Science and Graduate School, Mahidol University, Thailand.

References

[1] A. Artoli, J. Jenela and A. Sequeira, A comparative numerical study of a non-Newtonian blood flow model, Proc. IASME/WSEAS Int. Conf. on Continuum Mechanics, Greece, (2006), 91-96.

[2] A. D. Anastasiou, A. S. Spyrogianni, K. C. Koskinas, G. D. Giannoglou and S. V. Paras, Experimental investigation of the flow of a blood analogue fluid in a replica of a bifurcated small artery, Med. Eng. Phys. 34 (2012), 211-218.

[3] A. J. Bryan and G. D. Angelini, The biology of saphenous vein graft occlusion: Etiology and strategles for prevention, Curr. Opin. Cardiol. 9 (1994), 641-649.

[4] A. K. Chanitotis, L. Kaiktsis, D. Katritsis, E. Efstathopoulos, I. Pantos and V. Marmarellis, Computational study of pulsatile blood flow in prototype vessel geometries of coronary segments, Phys. Med. 26 (2010), 140-156.

[5] B. Nuntadilok, B. Wiwatanapataphee, M. Chuedoung and T. Siriapisith, Numerical simulation of blood flow in the system of human coronary arteries with and without bypass graft, Proc. 11th WSEAS Int. Conf. on System Science and Simulation in Engineering, Singapore, (2012), 43-48.

[6] B. Wiwatanapataphee, Modelling of non-Newtonian blood flow through stenosed coronary arteries, Dynamics of Continuous Discrete and Impulsive Systems Series B: Applications & Algorithms 15 (2008), 619-634.

[7] B. Wiwatanapataphee, D. Poltem, Y. H. Wu and Y. Lenbury, Simulation of pulsatile flow of blood in stenosed coronary artery bypass with graft, Math. Biosci. Eng. 3 (2006), 371-383.

[8] B. Wiwatanapataphee, S. Amornsamankul, Y. H. Wu and Y. Lenbury, Non-Newtonian blood flow through stenosed coronary arteries, Proc. 2nd WSEAS Int. Conf. on Applied and Theoretical Mechanics, Italy, (2006), 259-264.

[9] B. Wiwatanapataphee, Y. H. Wu, T. Siriapisith and B. Nuntadilok, Effect of branching on blood flow in the system of human coronary arteries, Math. Biosci. Eng. 9 (2012), 199-214.

[10] C. Bertolotti and V. Delplano, Three-dimensional numerical simulations of flow through a stenosed coronary bypass, J. Biomech. 33 (2000), 1011-1022.

[11] D. Tang, C. Yang, S. Kobayashi and D. N. Ku, Steady flow and wall compression in stenotic arteries: A three-dimensional thick-wall model with fluid-wall interactions, J. Biomech. Eng. 123(2) (2001), 548-557.

[12] E. Boutsianis, H. Dave, T. Frauenfelder, D. Poulikakos, S. Wildermuth, M. Turina, Y. Ventikos and G. Zund, Computational simulation of intracoronary flow based on real coronary geometry, Eur. J. Cardio-Thorac. 26 (2004), 248-256.

[13] E. Shaik, K. A. Hoffmann and J. F. Dietiker, Numerical simulation of pulsatile non-Newtonian flow in an end-to-side anastomosis model, Simul. Model. Pract. Th. 16 (2008), 1123-1135.

[14] J. Chen and X. Y. Lu, Numerical investigation of the non-Newtonian pulsatile blood flow in a bifurcation model with a non-planar branch, J. Biomech. 39 (2006), 818-832.

[15] J. Janela, A. Moura and A. Sequeira, A 3D non-Newtonian fluid-structure interaction model for blood flow in arteries, J. Comput. Appl. Math. 234 (2010), 2783-2791.

[16] J. V. Soulis, G. D. Giannoglou, Y. S. Chatzizisis, K. V. Seralidou, G. E. Parcharidis and G. E. Louridas, Non-Newtonian models for molecular viscosity and wall shear stress in a 3D reconstructed human left coronary artery, Med. Eng. Phys. 30 (2008), 9-19.

[17] N. J. Cheshire and J. H. Wolfe, Infrainguinal graft surveillance: A biased overview, Semin. Vasc. Surg. 6(2) (1993), 143-149.

[18] P. Chuchard, T. Puapansawat, T. Siriapisith, Y. H. Wu and B. Wiwatanapataphee, Numerical simulation of blood flow through the system of coronary arteries with diseased left anterior descending, Int. J. Math. Comput. Simulat. 5(4) (2011), 334-341.

[19] P. Chuchard, T. Puapansawat, T. Siriapisith and B. Wiwatanapataphee, Numerical simulation of blood flow in the system of human coronary arteries with stenosis, Proc. 4th WSEAS Int. Conf. on Finite Differences Finite Elements Finite Volumes Boundary Elements, France, (2011), 59-63.

[20] P. Ruengsakulrach, A. K. Joshi, S. Fremes, J. Butany, S. Foster, B. Wiwatanapataphee and Y. Lenbury, Wall shear stress and atherosclerosis: Numerical blood flow simulations in the mouse aortic arch, Proc. 12th WSEAS Int. Conf. on Applied Mathematics, Egypt, (2007), 199-207.

[21] R. Manimaran, CFD simulation of non-Newtonian fluid flow in arterial stenoses with surface irregularities, WASET 73 (2011), 957-962.

[22] S. I. Bernad, T. Barbat, E. S. Bernad and R. Susan-Resiga, Cardio vascular surgery simulation based medical intervention, Proc. 9th WSEAS Int. Conf. on Mathematics and Computers in Biology and Chemistry, Romania, (2008), 100-106.

[23] S. Sadeghian, M. Navidbakhsh and R. Molaei, Numerical flow analysis in actual model of human coronary, Proc. 3rd WSEAS Int. Conf. on Applied and Theoretical Mechanics, Spain, (2007), 131-135.

[24] S. U. Siddiqui, N. K. Verma, S. Mishra and R. S. Gupta, Mathematical modelling of pulsatile flow of Cassons fluid in arterial stenosis, Appl. Math. Comput. 210 (2009), 1-10.

[25] Y. Papaharilaou, D. J. Doorly and S. J. Sherwin, The influence of out-of-plane geometry on pulsatile flow within a distal end-to-side anastomosis, J. Biomech. 5(9) (2002), 1225-1239.

[26] Cleveland Clinic, Medical management of coronary artery disease. Available: http://my.clevelandclinic.org/heart/disorders/cad/treatment medical.aspx

[27] World Health Organization (WHO), Cardiovascular Diseases (CVDs). Available: http://www.who.int/mediacentre/factsheets/fs317/en/

■